On the relation between deposition rate and ionized flux fraction in high power impulse magnetron sputtering

Jón Tómas Guðmundsson[1,2], Hamid Hajihoseini[1,2], Martin Rudolph[3], Nils Brenning[1,4,5], Michael A. Raadu[1], Tiberiu M. Minea[4], and Daniel Lundin[4,5,6]

[1] Department of Space and Plasma Physics, KTH Royal Institute of Technology, Stockholm, Sweden
[2] Science Institute, University of Iceland, Reykjavik, Iceland
[3] Leibniz Institute of Surface Engineering (IOM), Permoserstraße 15, 04318 Leipzig, Germany
[4] Laboratoire de Physique des Gaz et Plasmas - LPGP, CNRS, Université Paris-Sud, Orsay, France
[5] Plasma and Coatings Physics, IFM-Materials Physics, Linköping University, Sweden
[6] Ionautics AB, Linköping, Sweden

Introduction

- Magnetron sputtering discharges are widely used for thin film deposition – spanning various industries
- In the planar circular configuration it is simply a diode discharge with two concentric stationary cylindrical magnets placed directly behind the cathode target

- Applications include deposition of
  - thin films in integrated circuits
  - magnetic material
  - hard, protective, and wear resistant coatings
  - optical coatings
  - decorative coatings
  - low friction films

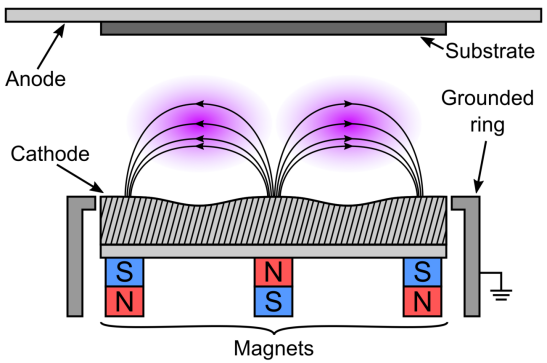

Gudmundsson and Lundin (2020) in High Power Impulse Magnetron Sputtering Discharge, Elsevier, 2020

Introduction

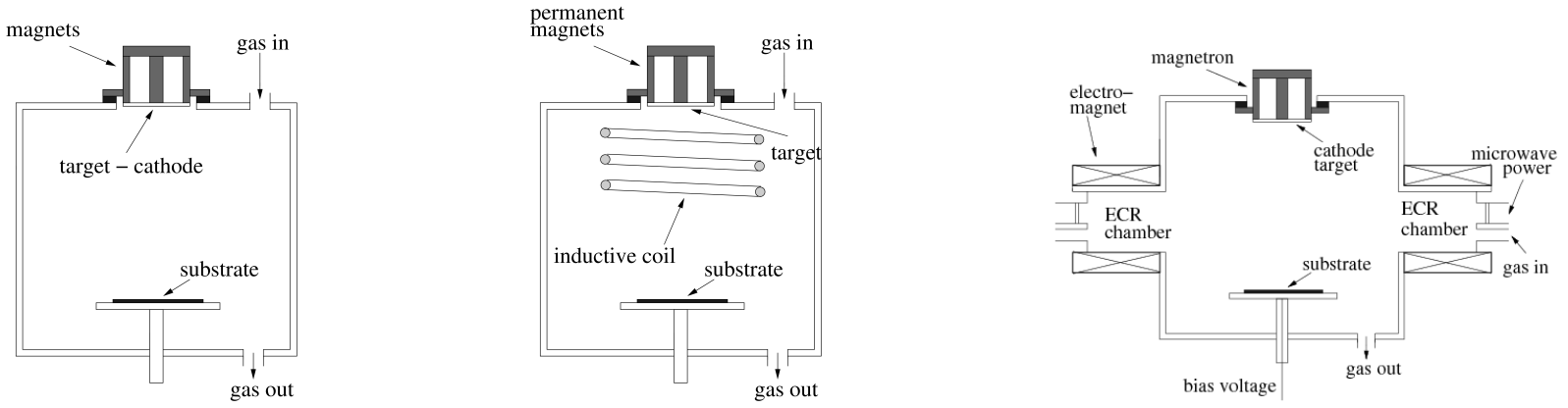

From Gudmundsson (2008) J. Phys.: Conf. Ser. **100** 082002

- A typical dc planar magnetron discharge operates at a pressure of 1 – 10 mTorr with a magnetic field strength of 10 – 50 mT and at cathode potentials 300 – 700 V
- Electron density in the substrate vicinity is in the range $10^{15} - 10^{16}$ m^{-3}
  - low fraction of the sputtered material is ionized ($\sim$ 1 %)
  - the majority of ions are the ions of the inert gas
  - additional ionization by a secondary discharge (rf or microwave)

Gudmundsson (2020) PSST **29**(11) 113001

Introduction

- High ionization of sputtered material requires very high density plasma
- In a conventional dc magnetron sputtering discharge the power density (plasma density) is limited by the thermal load on the target
- High power pulsed magnetron sputtering (HPPMS)
- In a HiPIMS discharge a high power pulse is supplied for a short period
  - low frequency
  - low duty cycle
  - low average power

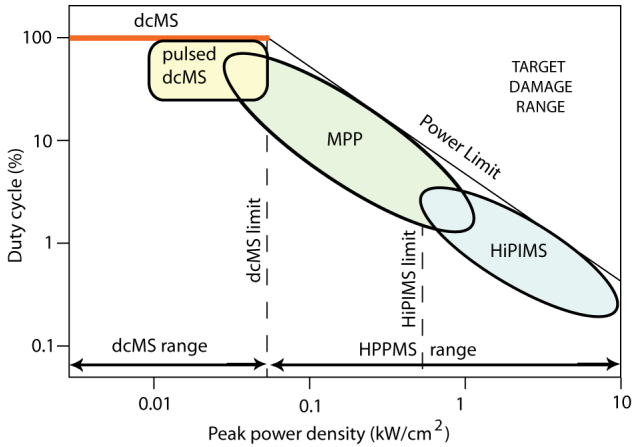

Gudmundsson et al. (2012) JVSTA **30** 030801

- Power density limits
  $p_t = 0.05$ kW/cm^2 dcMS limit
  $p_t = 0.5$ kW/cm^2 HiPIMS limit

Introduction

- Temporal and spatial variation of the electron density in HiPIMS discharge
- Ar discharge at 20 mTorr, Ti target, pulse length 100 μs
- The electron density in the substrate vicinity is of the order of $10^{18} - 10^{19}$ m^{-3}
- The electron density versus the discharge current density measured in dc diode and magnetron sputtering discharges

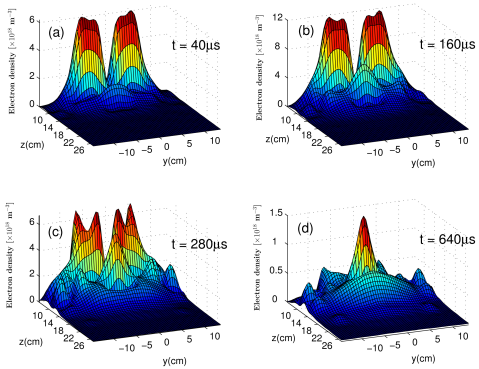

Bohlmark et al. (2005), IEEE Trans. Plasma Sci. **33** 346

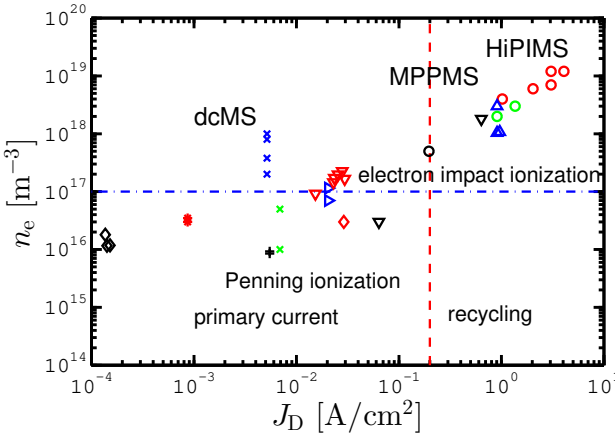

From Gudmundsson (2020) PSST **29**(11) 113001

Thin film deposition

Thin film deposition – Fraction of ionization

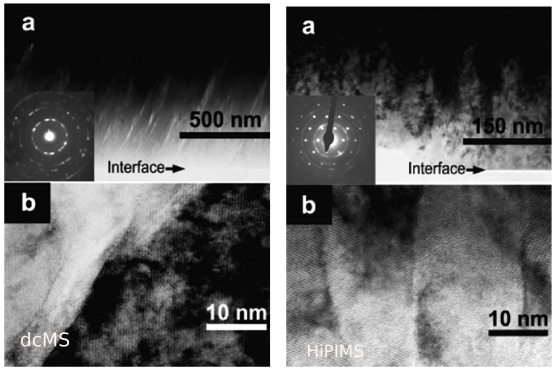

Alami et al. (2005) JVSTA **23** 278

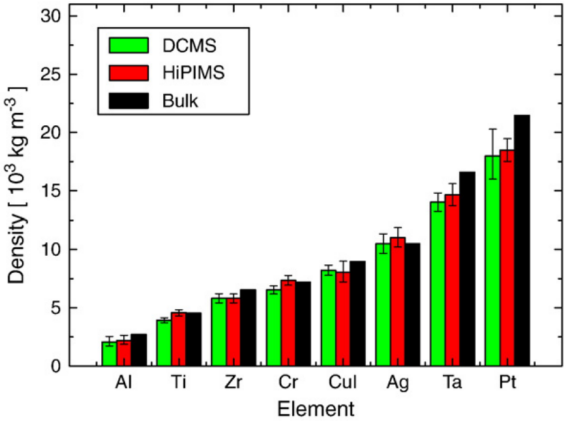

From Samuelsson et al. (2010) SCT **202** 591

- In HiPIMS deposition, the high fraction of ionization of the sputtered species has been shown to lead to
  - growth of smooth and dense films
  - enable control over their phase composition and microstructure
  - enhance mechanical, electrical, and optical properties
  - improve film adhesion
  - enable deposition of uniform films on complex-shaped substrates
- The mass density is always higher and the surfaces are significantly smoother when depositing with HiPIMS compared to dcMS at the same average power

Thin film deposition – Film Resistivity

- TiN as diffusion barriers for copper and aluminum interconnects
- HiPIMS deposited films have significantly lower resistivity than dcMS deposited films on SiO_2 at all growth temperatures due to reduced grain boundary scattering
- Thus, ultrathin continuous TiN films with superior electrical characteristics and high resistance towards oxidation can be obtained with HiPIMS at reduced temperatures

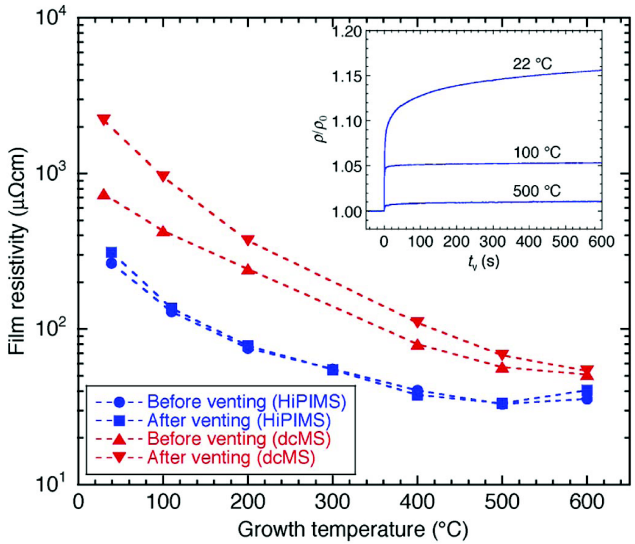

From Magnus et al. (2012) IEEE EDL **33** 1045

Thin film deposition – Molecular Dynamics simulation

- The effect of ionization fraction on the epitaxial growth of Cu film on Cu(111) substrate explored using Molecular Dynamics simulation
- Three deposition methods
  - thermal evaporation, fully neutral
  - dcMS, 50 % ionized
  - HiPIMS, 100 % ionized
- Higher ionization fraction of the deposition flux leads to smoother surfaces by two major mechanisms
  - decreasing clustering in the vapor phase
  - bicollision of high energy ions at the film surface that prevents island growth to become dominant

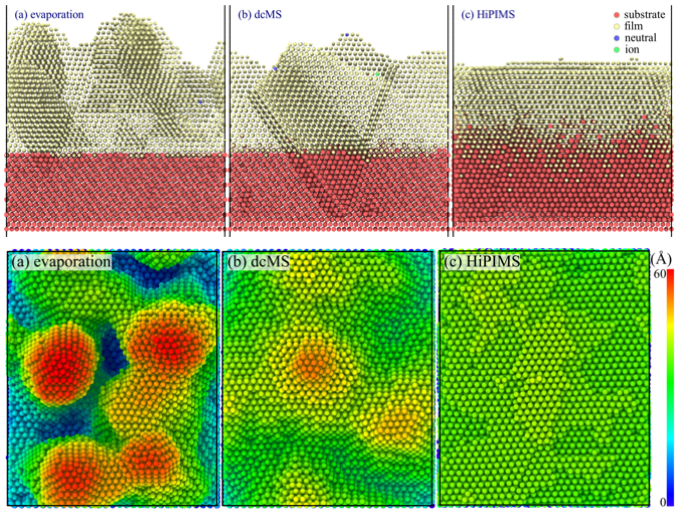

After Kateb et al. (2019) JVSTA **37** 031306

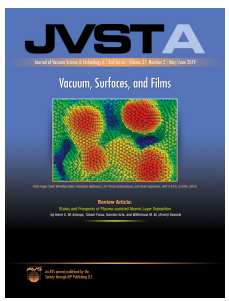

Thin film deposition – Deposition rate

- There is a drawback
- The deposition rate is lower for HiPIMS when compared to dcMS operated at the same average power
- The HiPIMS deposition rates are typically in the range of 30 – 85% of the dcMS rates depending on target material
- Many of the ions of the target material are attracted back to the target surface by the cathode potential

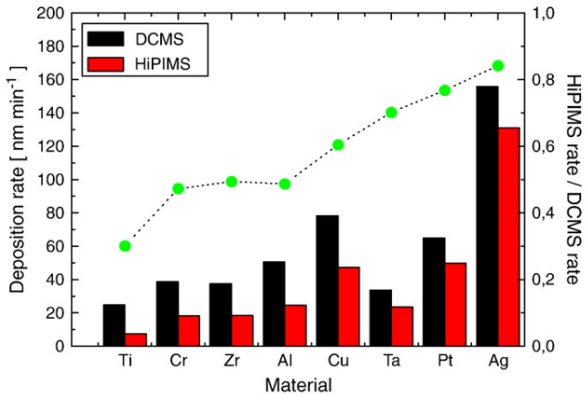

From Samuelsson et al. (2010) SCT **202** 591

Introduction – Fraction of ionization

- Quantification and control of the fraction of ionization of the sputtered species are crucial in magnetron sputtering
- We distinguish between three approaches to describe the degree (or fraction) of ionization
  - the ionized flux fraction

$$F_{\text{flux}} = \frac{\Gamma_{\text{i}}}{\Gamma_{\text{i}} + \Gamma_{\text{n}}}$$

  - the ionized density fraction

$$F_{\text{density}} = \frac{n_{\text{i}}}{n_{\text{i}} + n_{\text{n}}}$$

  - the fraction α_{t} of the sputtered metal atoms that become ionized in the plasma (probability of ionization)

Butler et al. (2018) PSST **27** 105005

Influence of magnetic field

Influence of magnetic field

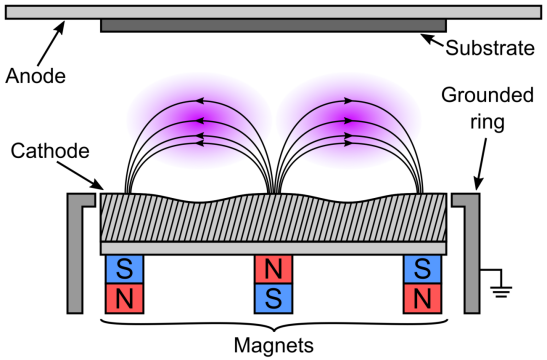

Gudmundsson and Lundin (2020) in High Power Impulse Magnetron Sputtering Discharge, Elsevier, 2020

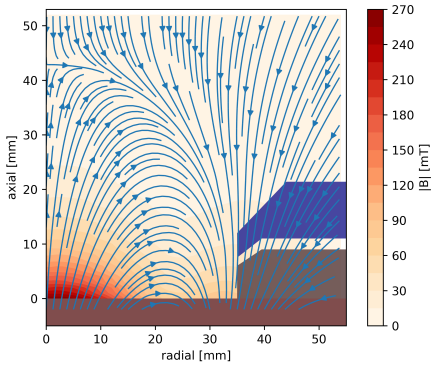

Figure provided by Zanáška and Mainwaring (2020)

- The magnetron sputtering discharge is based on magnetic confinement of the electrons
- To describe the magnetic field we use
  - The magnetic field strength just above the race track denoted by $B_{\mathrm{rt}} = |\mathbf{B}|$
  - The magnetic null point, which is the distance from the target surface to the point where the magnetic flux density changes its direction and is denoted by z_{null}

Influence of magnetic field – Deposition rate

- The Ti deposition rate and the ionized flux fraction are measured using a gridless ion meter (m-QCM)

  Kubart et al. (2014) *SCT* **238** 152

- The ion meter is mounted on a probe holder which can be moved around within the chamber
- The Ar working gas pressure was set to 1 Pa
- In all cases the pulse width was 100 μs at an average power of 300 W

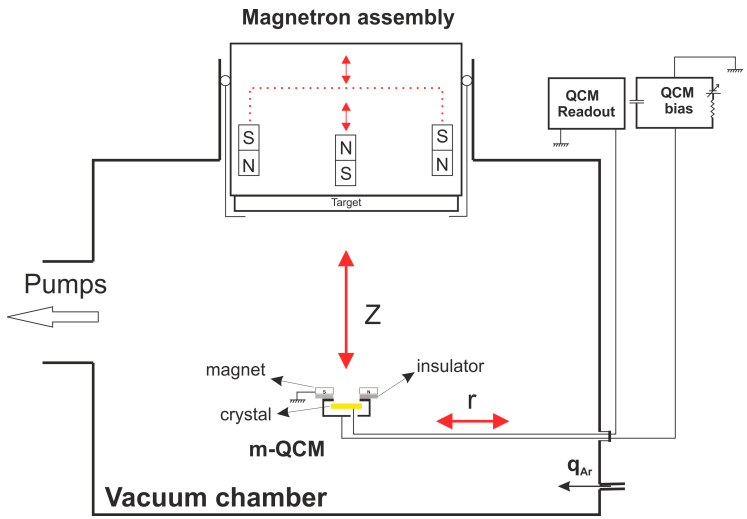

From Hajihoseini et al. (2019) *Plasma* **2** 201

Influence of magnetic field – Deposition rate

- The Ti deposition rate recorded at substrate position using a gridless ion meter (m-QCM)
  - **dcMS**
    +10% with decreasing $|\mathbf{B}|$
    (but no obvious trend)
  - **HiPIMS fixed voltage**
    +110% with decreasing $|\mathbf{B}|$
  - **HiPIMS fixed peak current**
    +40% with decreasing $|\mathbf{B}|$
- In HiPIMS operation the deposition rate increases with decreasing $|\mathbf{B}|$, ordered from high $|\mathbf{B}|$ at the left to low $|\mathbf{B}|$ on the right

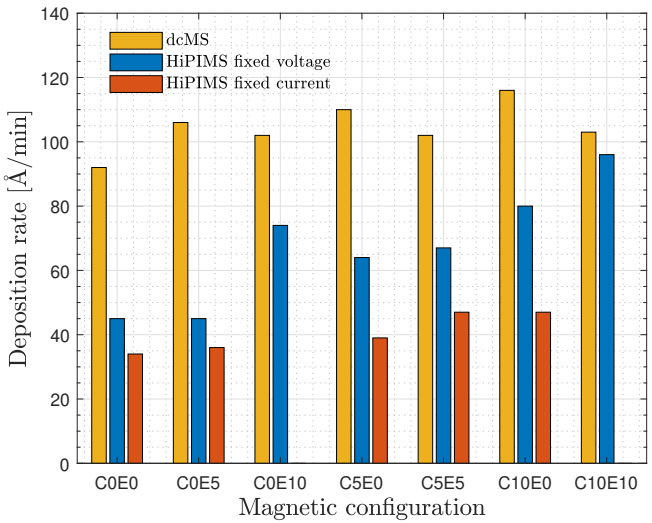

From Hajihoseini et al. (2019) *Plasma* **2** 201

Influence of magnetic field – Ionized flux fraction

- Ionized flux fraction recorded
  - **dcMS**
    Always around 0 %
    (Kubart et al., 2014)
  - **HiPIMS fixed voltage**
    -75% with decreasing $|\mathbf{B}|$
  - **HiPIMS fixed peak current**
    $+50\%$ with decreasing $|\mathbf{B}|$
- The ionized flux fraction decreases with decreasing $|\mathbf{B}|$ when the HiPIMS discharge is operated in fixed voltage mode but increases in fixed peak current mode
- Opposing trends

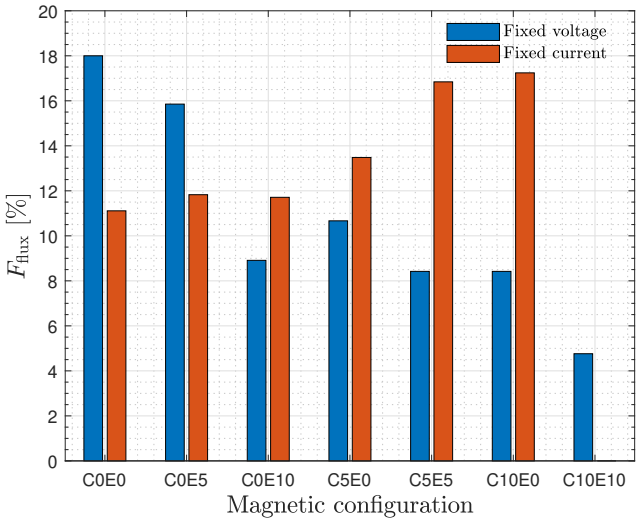

From Hajihoseini et al. (2019) *Plasma* **2** 201

Influence of magnetic field – Ionized flux fraction

- The total radial material flux across the side surface of a cylinder divided by the total axial flux of the film forming material across the top circular surface at $z = 70$ mm
- The total radial flux of the film forming material is often greater in dcMS compared to HiPIMS
- Therefore the reduction of the (axial) deposition rate in HiPIMS compared to dcMS is not due to increased radial transport in HiPIMS

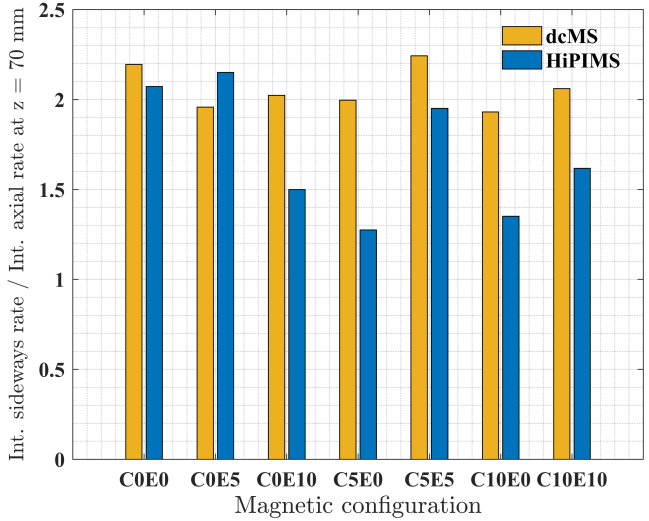

From Hajihoseini et al. (2020) *JVSTA* **38** 033009

Influence of magnetic field – Ionized flux fraction

- The ratio of sideways ion deposition rate at $(r, z) = (50, 35)$ mm and the axial rate at $(r, z) = (0, 70)$ mm for the seven magnet configurations
- The magnet configurations on the x-axis are ordered from high $|\mathbf{B}|$ at the left to low $|\mathbf{B}|$ on the right
- The radial ion deposition rate is at least as large as the axial ion deposition rate, and often around two times higher

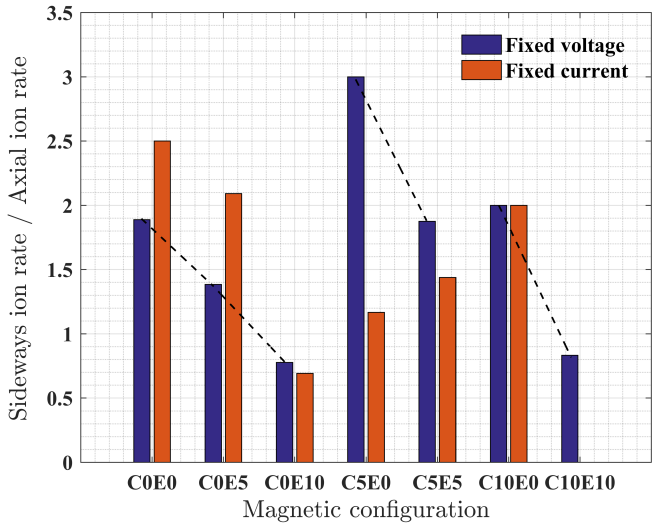

From Hajihoseini et al. (2020) *JVSTA* **38** 033009

Internal parameters and optimization

Influence of magnetic field – α_t and β_t

- Low deposition rate is the main drawback of this sputter technology and hampers its use for industrial applications
- The main reason for the low deposition rate of the HiPIMS discharge is suggested to be due to the back-attraction of the ions of the sputtered species to the cathode target
- This process is described by two parameters
  - α_t – ionization probability
  - β_t – back-attraction probability
- Increased deposition rate in HiPIMS often comes at the cost of a lower ionized flux fraction of the sputtered material

Influence of magnetic field – α_t *and* β_t

- We can relate the measured quantities deposition rate $F_{\mathrm{DR,sput}}$ and the ionized flux fraction $F_{\mathrm{ti,flux}}$

$$F_{\mathrm{DR,sput}} = \frac{\Gamma_{\mathrm{DR}}}{\Gamma_0} = (1 - \alpha_t \beta_t)$$

$$F_{\mathrm{ti,flux}} = \frac{\Gamma_{\mathrm{DR,ions}}}{\Gamma_{\mathrm{DR,sput}}} = \frac{\Gamma_0 \alpha_t (1 - \beta_t)}{\Gamma_0 (1 - \alpha_t \beta_t)} = \frac{\alpha_t (1 - \beta_t)}{(1 - \alpha_t \beta_t)}$$

to the internal parameters back attraction probability β_t

$$\beta_t = \frac{1 - F_{\mathrm{DR,sput}}}{1 - F_{\mathrm{DR,sput}}(1 - F_{\mathrm{ti,flux}})}$$

and ionization probability α_t

$$\alpha_t = 1 - F_{\mathrm{DR,sput}}(1 - F_{\mathrm{ti,flux}})$$

Internal parmeters – α_t and β_t refined

- The particle fluxes out of the diffusion region and the fluxes onto the ion meter are related by the transport parameters ξ_{tn} and ξ_{ti} for neutrals and ions, and these are in general not equal:
  - A larger scattering cross-section for ions compared to neutrals
  - Ions are influenced by the electric fields in the IR
  - Plasma instabilities such as spokes further broaden the scatter cone of target ions
- The resulting angular distributions of neutrals and ions are shown schematically

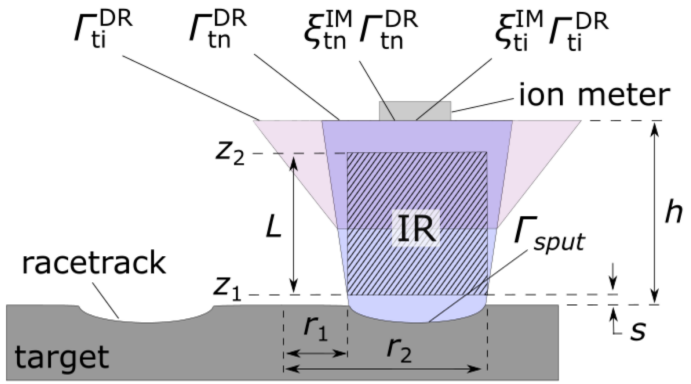

Rudolph et al. (2020) *JAP*

submitted November 2020

Internal parmeters – α_t and β_t refined

- The ionization probability of the sputtered species is then

$$\alpha_t = 1 - F^{IM}_{sput \rightarrow IM}(1 - F^{IM}_{ti,flux})$$

and the ion back-attraction probability

$$\beta_t = \frac{F^{IM}_{sput \rightarrow IM} F^{IM}_{ti,flux} \left(1 - \frac{\xi_{tn}}{\xi_{ti}}\right) - F^{IM}_{sput \rightarrow IM} + 1}{1 - F^{IM}_{sput \rightarrow IM}(1 - F^{IM}_{ti,flux})}$$

which is a more general form of the equations for α_t and β_t than used earlier and assumed $\xi_{tn} = \xi_{ti}$

- We find $\xi_{tn}/\xi_{ti} \approx 1.9$

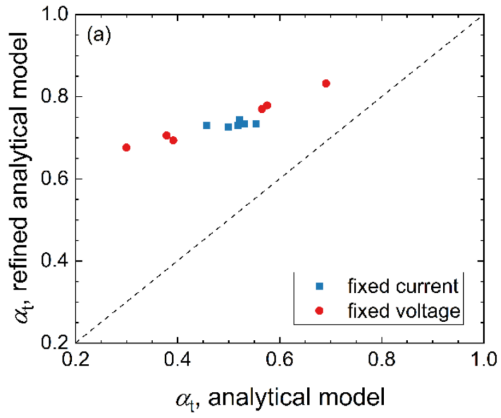

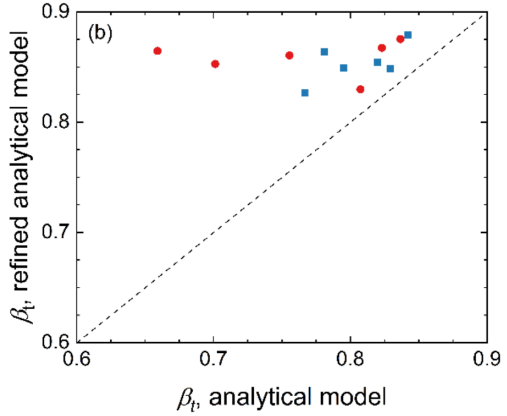

Rudolph et al. (2020) *JAP* submitted November 2020

Internal parmeters – α_t and β_t refined

- The results of the refined analytical model have also been validated using the IRM, a global volume averaged plasma-chemistry model based on particle and power balance

Huo et al. (2017) JPD **50** 354003

- The IRM is fitted according to a well-described procedure using the measured ionized flux fraction and the measured discharge current and voltage waveforms
- The IRM volume is assumed to be defined by $r_1 = 11$ mm, $r_2 = 39$ mm, $z_1 = 2$ mm and $z_2 = 25$ mm

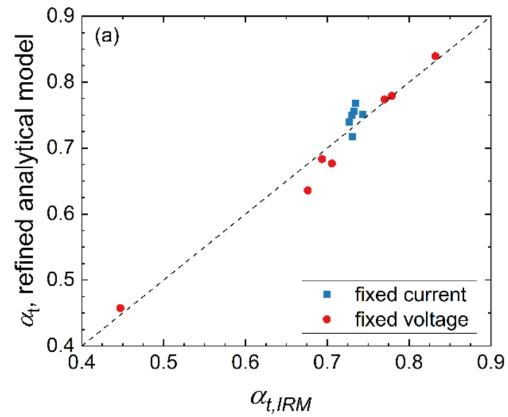

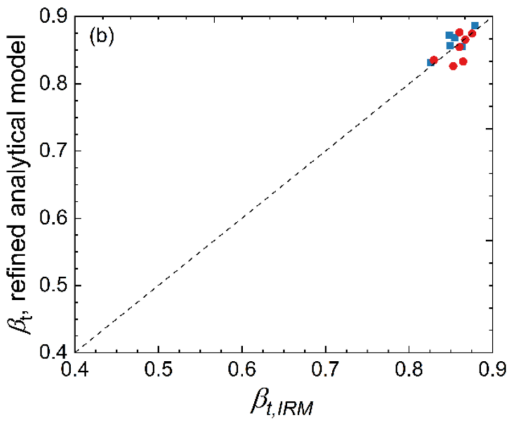

Rudolph et al. (2020) *JAP* submitted November 2020

Influence of magnetic field – Optimization

- There are two measures of how good a HiPIMS discharge is:
  - the fraction $F_{\mathrm{DR,sput}}$ of all the sputtered material that reaches the diffusion region (DR)
  - the fraction $F_{\mathrm{ti,flux}}$ of ionized species in that flux
- There is a trade off between the goals of higher $F_{\mathrm{DR,sput}}$ and higher $F_{\mathrm{ti,flux}}$
- The figure shows $F_{\mathrm{DR,sput}}$ and $F_{\mathrm{ti,flux}}$ as functions of α_{t} at assumed fixed value of $\beta_{\mathrm{t}} = 0.87$

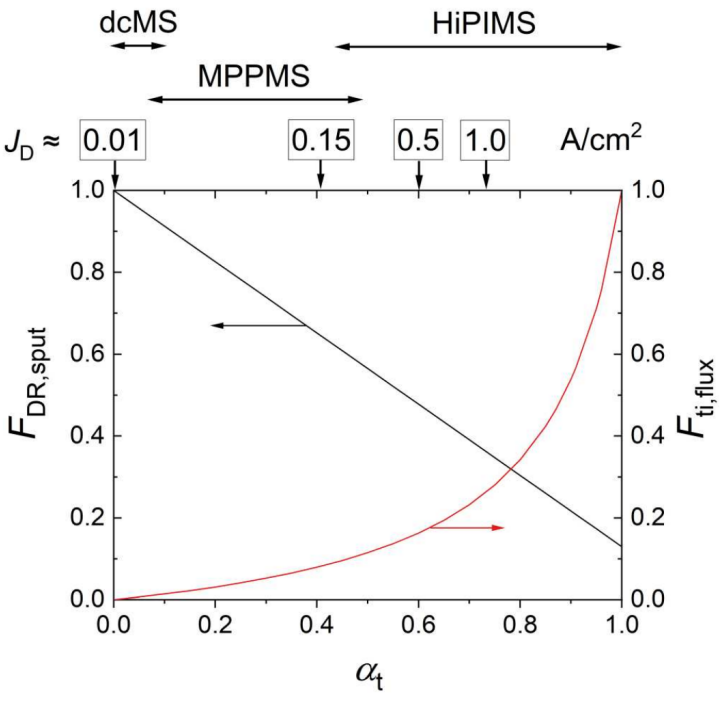

From Brenning et al. (2020) *JVSTA* **38** 033008

Influence of magnetic field – Optimization

- For a particular application an ionized flux fraction of 30 % is suitable but $0.8 \leq \beta_t \leq 0.95$
- Following the green dotted line from the value $F_{\mathrm{ti,flux}} = 0.30$ to the red dashed curve gives $\alpha_t = 0.9$ (red square)
- The black dashed line then shows α_t only 15 % of the total sputtered flux enters the diffusion region ($F_{\mathrm{DR,sput}} = 0.15$).
- Solid lines show that reducing the back-attraction to $\beta_t = 0.8$ where $\alpha_t = 0.69$ is sufficient to maintain $F_{\mathrm{ti,flux}} = 0.30$ (red circle) and $F_{\mathrm{DR,sput}} = 0.45$ or a factor of three increase in the deposition rate

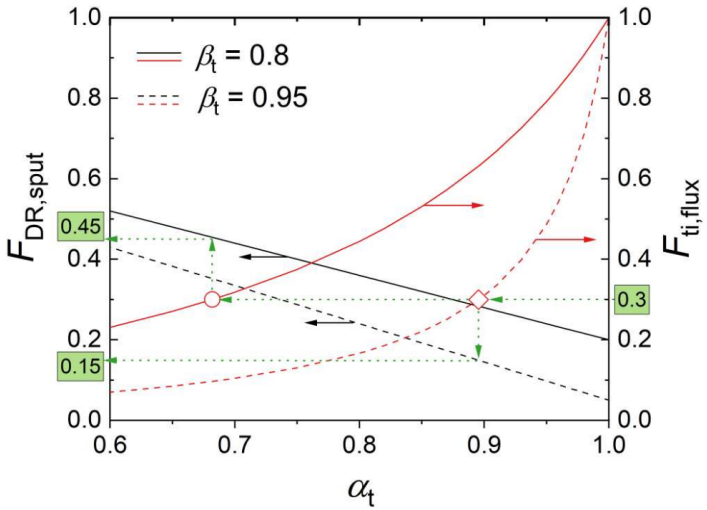

From Brenning et al. (2020) *JVSTA* **38** 033008

Influence of magnetic field – α_t and β_t

- When operating in the fixed voltage mode (**red**) the ionization probability α_t increases with increased magnetic field strength – which is essentially the discharge current
- When operating in the fixed peak current mode (**black**) the ionization probability α_t is roughly constant independent of the magnetic field strength
- α_t can be varied in the range $0 \leq \alpha_t \leq 1$ by the discharge current amplitude J_D
- β_t is variable within a much smaller achievable range and depends heavily on the magnetic field strength

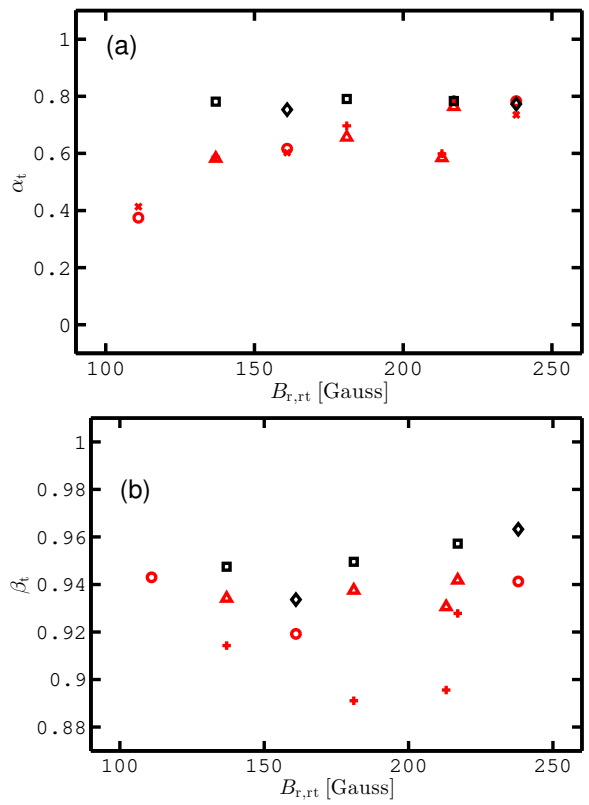

From Hajihoseini et al. (2019) *Plasma* 2 201

Influence of magnetic field – α_t and β_t

- The figure shows β_t as a function of the magnetic field strength (measured 11 mm above the racetrack center)
- There is a clear trend that β_t is lowered when the magnetic field strength is reduced
- Using the line fit, we find that β_t = 0.96 for the highest magnetic field strength and β_t = 0.93 for the lowest magnetic field strength
- Our proposed figure of merit $(1 - \beta_t)$ changes by a factor of $(1 - 0.93)/(1 - 0.96) = 1.8$

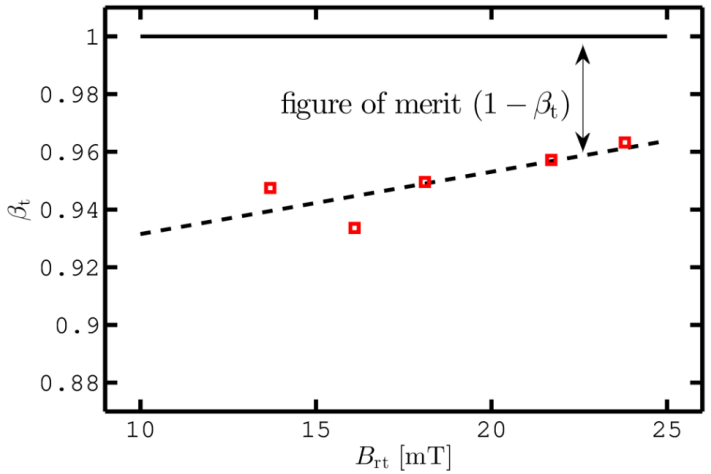

From Brenning et al. (2020) *JVSTA* **38** 033008

Influence of magnetic field – α_t and β_t

- The internal discharge parameters from the IRM
- The ionization probability α_t versus the discharge current
- The ion escape fraction $(1 - \beta_t)$ versus the magnetic field strength

From Rudolph et al. (2021a) manuscript in preperation

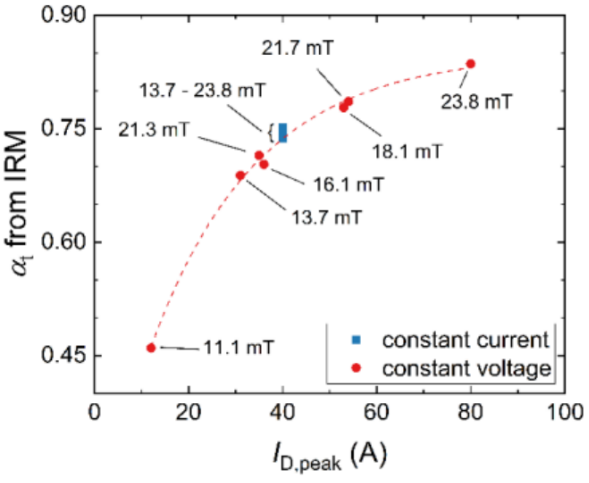

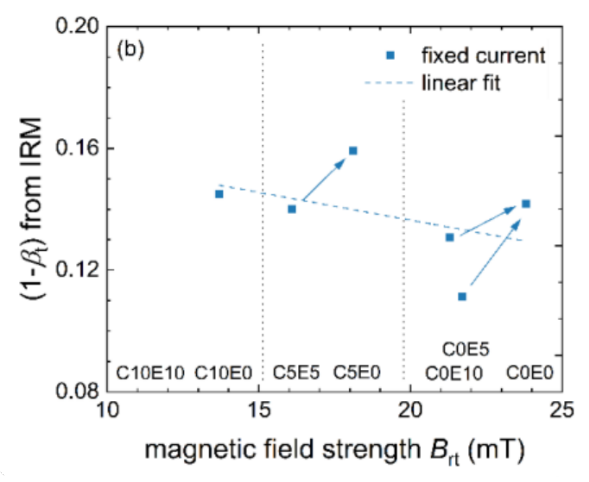

Influence of magnetic field – Pulse length

- For the same average power, shorter pulse lengths give higher deposition rate than with longer pulse lengths
- The same average power can simply be achieved by increasing the frequency
- Shortening the pulses does not affect the ionized flux fraction, which remains essentially constant
  - with shorter pulses, the afterglow contributes increasingly more to the total deposition rate
  - the ionized flux fraction from the afterglow is typically higher compared to that during the pulse due to absent back-attracting electric field

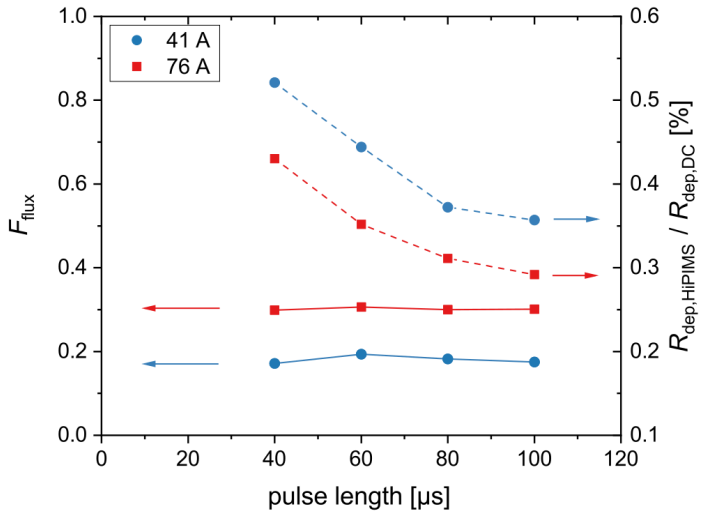

From Rudolph et al. (2020) *PSST* **29** 05LT01

Influence of magnetic field – Pulse length

- For the same average power, shorter pulse lengths give higher deposition rate than with longer pulse lengths
- The same average power can simply be achieved by increasing the frequency
- Shortening the pulses does not affect the ionized flux fraction, which remains essentially constant
  - with shorter pulses, the afterglow contributes increasingly more to the total deposition rate
  - the ionized flux fraction from the afterglow is typically higher compared to that during the pulse due to absent back-attracting electric field

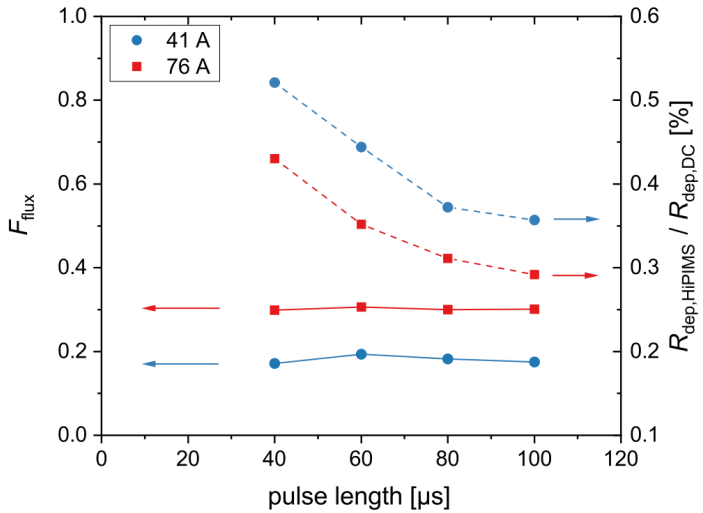

From Rudolph et al. (2020) *PSST* **29** 05LT01

Influence of magnetic field – Pulse length

- By switching-off the cathode potential during the afterglow decreases the effective β_t
- β_t decreases with decreasing pulse length
- The relative contribution of the afterglow ions to the flux toward the DR increases steadily for shorter pulses
- The ionization probability α_t also decreases with a shorter pulse length
- The useful fraction of the sputtered species

$$F_{DR,sput} = \frac{\Gamma_{DR}}{\Gamma_0} = (1 - \alpha_t \beta_t)$$

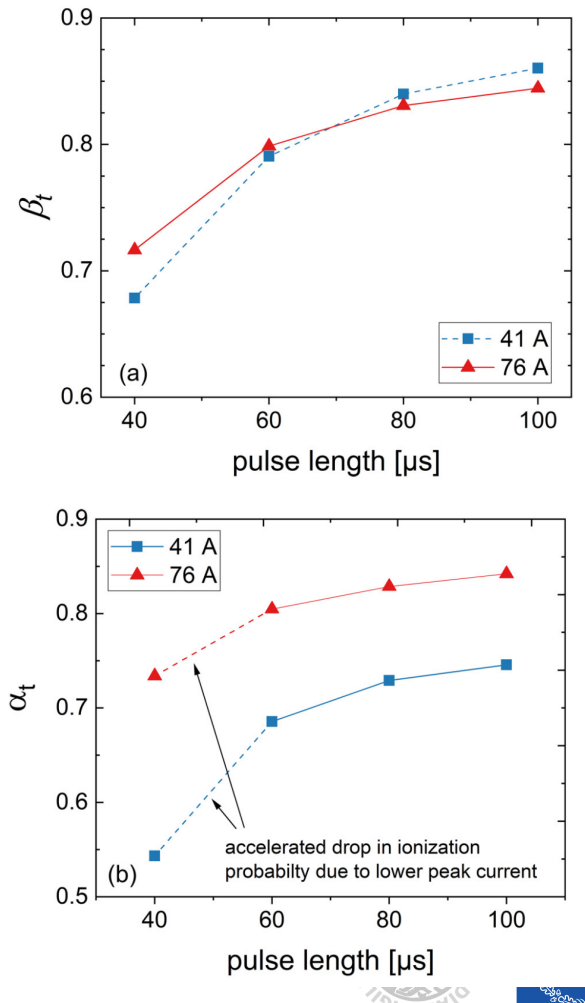

From Brenning et al. (2020) *JVSTA* **38** 033008

Influence of magnetic field – Pulse length

- HiPIMS can be optimized by selecting
  - pulse power
  - pulse length
  - working gas pressure
  - magnetic field strength
- The HiPIMS compromise – a fully ionized material flux is not required to achieve significant improvement of the thin film properties
- A sufficiently high peak discharge current is required to reach the desired ionized flux fraction
- Further increase would lead to unnecessarily low deposition rates

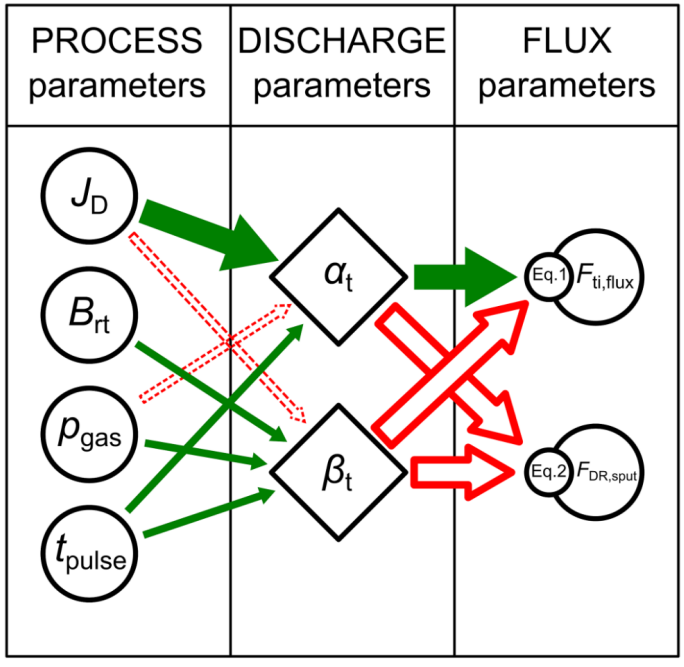

From Brenning et al. (2020) *JVSTA* **38** 033008

Mixed high power and low power pulsing

- The HiPIMS discharge can also be optimized by mixing two different power levels in the pulse pattern
  - Standard HiPIMS pulses create the ions of the film-forming material
  - An off-time follows, during which no voltage (or a reversed voltage) to let ions escape towards the substrate
  - Then long second pulse, in the dc magnetron sputtering range, is applied, to create neutrals of the film-forming material
- The optimum power split is decided by the lowest ionized flux fraction that gives the desired film properties for a specific application

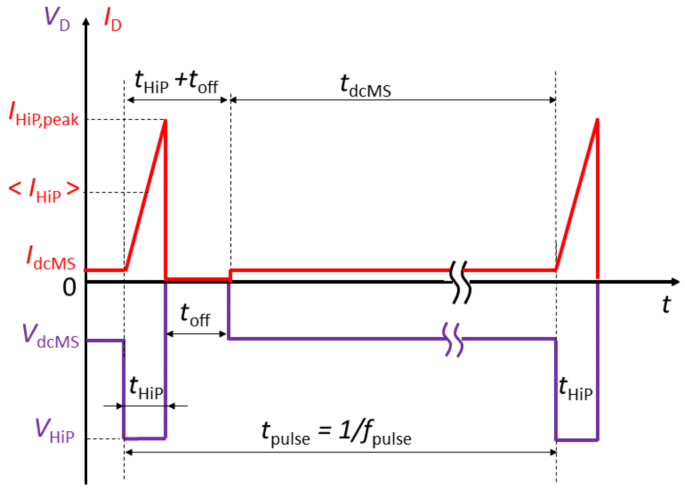

Brenning et al. (2020) *PSST*

submitted September 2020

Electron energy distribution function

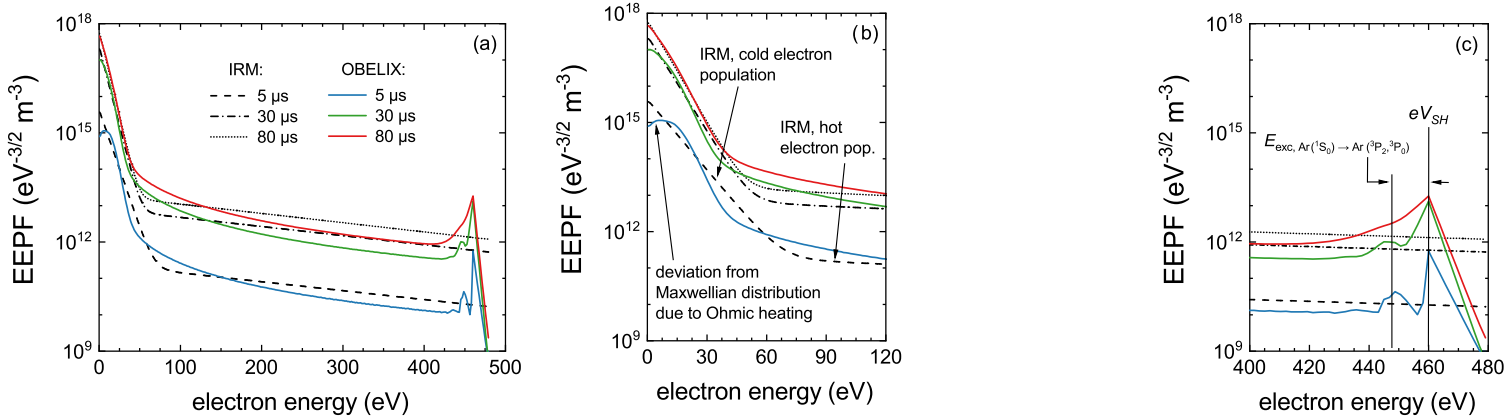

- The electron energy probability function (EEPF) at different times in the discharge pulse (pulse initiation (5 μs), current rise (20 μs), and plateau region (80 μs)) for a discharge with a 4 inch titanium target and operated with a peak discharge current of $I_{\mathrm{D,peak}}$ = 41 A
- A very good agreement between the bi-Maxwellian EEDF assumed by the IRM and the EEDF that is calculated self-consistently using the OBELIX model - a Boltzmann solver

From Rudolph et al. (2021b) manuscript in preperation

Summary

Summary

- For HiPIMS in the fixed voltage mode: A trade-off between the deposition rate (increases by more than a factor of two) and the ionized flux fraction (decreases by a factor 4 to 5) with decreasing $|\mathbf{B}|$
- For HiPIMS in the fixed peak current mode: Decreasing $|\mathbf{B}|$ improves both the deposition rate (by 40%) and the ionized flux fraction (by 50%)
- There is an inescapable conflict between the goals of higher deposition rate and higher fraction of ionized species in the sputtered material flux
- The HiPIMS discharge can be optimized by adjusting the pulse power, pulse length, working gas pressure and the magnetic field strength

Thank you for your attention

The slides can be downloaded at
`http://langmuir.raunvis.hi.is/~tumi/ranns.html`
and the project is funded by

- Icelandic Research Fund Grant Nos. 130029 and 196141

References

Alami, J., P. O. A. Petersson, D. Music, J. T. Gudmundsson, J. Bohlmark, and U. Helmersson (2005). Ion-assisted physical vapor deposition for enhanced film deposition on non-flat surfaces. *Journal of Vacuum Science and Technology A 23*(2), 278–280.

Bohlmark, J., J. T. Gudmundsson, J. Alami, M. Lattemann, and U. Helmersson (2005). Spatial electron density distribution in a high-power pulsed magnetron discharge. *IEEE Transactions on Plasma Science 33*(2), 346–347.

Brenning, N., A. Butler, H. Hajihoseini, M. Rudolph, M. A. Raadu, J. T. Gudmundsson, T. Minea, and D. Lundin (2020). Optimization of HiPIMS discharges: The selection of pulse power, pulse length, gas pressure, and magnetic field strength. *Journal of Vacuum Science and Technology A 38*(3), 033008.

Brenning, N., H. Hajihoseini, M. Rudolph, M. A. Raadu, J. T. Gudmundsson, T. M. Minea, and D. Lundin (2020). Hipims optimization by using mixed high-power and low-power pulsing. *Plasma Sources Science and Technology*, submitted September 2020.

Butler, A., N. Brenning, M. A. Raadu, J. T. Gudmundsson, T. Minea, and D. Lundin (2018). On three different ways to quantify the degree of ionization in sputtering magnetrons. *Plasma Sources Science and Technology 27*(10), 105005.

Gudmundsson, J. T. (2008). Ionized physical vapor deposition (IPVD): Magnetron sputtering discharges. *Journal of Physics: Conference Series 100*, 082002.

Gudmundsson, J. T. (2020). Physics and technology of magnetron sputtering discharges. *Plasma Sources Science and Technology 29*(11), 113001.

Gudmundsson, J. T., N. Brenning, D. Lundin, and U. Helmersson (2012). The high power impulse magnetron sputtering discharge. *Journal of Vacuum Science and Technology A 30*(3), 030801.

Gudmundsson, J. T. and D. Lundin (2020). Introduction to magnetron sputtering. In D. Lundin, T. Minea, and J. T. Gudmundsson (Eds.), *High Power Impulse Mangetron Sputtering: Fundamentals, Technologies, Challenges and Applications*, pp. 1–48. Amsterdam, The Netherlands: Elsevier.

Hajihoseini, H., M. Čada, Z. Hubička, S. Ünaldi, M. A. Raadu, N. Brenning, J. T. Gudmundsson, and D. Lundin (2019). The effect of magnetic field strength and geometry on the deposition rate and ionized flux fraction in the HiPIMS discharge. *Plasma 2*(2), 201–221.

References

Hajihoseini, H., M. Čada, Z. Hubička, S. Ünaldi, M. A. Raadu, N. Brenning, J. T. Gudmundsson, and D. Lundin (2020). Sideways deposition rate and ionized flux fraction in dc and high power impulse magnetron sputtering. *Journal of Vacuum Science and Technology A 38*(3), 033009.

Huo, C., D. Lundin, J. T. Gudmundsson, M. A. Raadu, J. W. Bradley, and N. Brenning (2017). Particle-balance models for pulsed sputtering magnetrons. *Journal of Physics D: Applied Physics 50*(35), 354003.

Kateb, M., H. Hajihoseini, J. T. Gudmundsson, and S. Ingvarsson (2019). Role of ionization fraction on the surface roughness, density, and interface mixing of the films deposited by thermal evaporation, dc magnetron sputtering, and HiPIMS: An atomistic simulation. *Journal of Vacuum Science and Technology A 37*(3), 031306.

Kubart, T., M. Čada, D. Lundin, and Z. Hubička (2014). Investigation of ionized metal flux fraction in HiPIMS discharges with Ti and Ni targets. *Surface and Coatings Technology 238*, 152–157.

Magnus, F., A. S. Ingason, S. Olafsson, and J. T. Gudmundsson (2012). Nucleation and resistivity of ultrathin TiN films grown by high power impulse magnetron sputtering. *IEEE Electron Device Letters 33*(7), 1045 – 1047.

Rudolph, M., N. Brenning, M. A. Raadu, H. Hajihoseini, J. T. Gudmundsson, A. Anders, and D. Lundin (2020). Optimizing the deposition rate and ionized flux fraction by tuning the pulse length in high power impulse magnetron sputtering. *Plasma Sources Science and Technology 29*(5), 05LT01.

Rudolph, M., H. Hajihoseini, M. A. Raadu, J. T. Gudmundsson, N. Brenning, T. M. Minea, A. Anders, and D. Lundin (2020). On how to measure the probabilities of target atom ionization and target ion back-attraction in high-power impulse magnetron sputtering. *Journal of Applied Physics*, submitted November 2020.

Samuelsson, M., D. Lundin, J. Jensen, M. A. Raadu, J. T. Gudmundsson, and U. Helmersson (2010). On the film density using high power impulse magnetron sputtering. *Surface and Coatings Technology 202*(2), 591–596.

Zanáška, M. and D. Mainwaring (2020). Personal communication, March 2020. The data was measured at Linköping University, Sweden, using a Gencoa magnetron assembly.